Received: 18 September 2024 | Revised: 21 December 2024 | Accepted: 7 January 2025

DOI: 10.1111/ppl.70089

ORIGINAL RESEARCH

Physiologia Plantarum

Inositol polyphosphates regulate resilient mechanisms in the green alga *Chlamydomonas reinhardtii* to adapt to extreme nutrient conditions

Rodrigo Bedera-García | **María Elena García-Gómez** | **José María Personat** | **Inmaculada Couso**

Institute for Plant Biochemistry and Photosynthesis, Consejo Superior de Investigaciones Científicas, Seville, Spain

Correspondence
Inmaculada Couso,
Email: inmaculada.couso@ibvf.csic.es

Funding information
Ministerio de Ciencia, Innovación y Universidades, Grant/Award Number: FPU22/00688

Edited by E. Monte

Abstract

In the context of climate changing environments, microalgae can be excellent organisms to understand molecular mechanisms that activate survival strategies under stress. *Chlamydomonas reinhardtii* signalling mutants are extremely useful to decipher which strategies photosynthetic organisms use to cope with changeable environments. The mutant *vip1-1* has an altered profile of pyroinositol polyphosphates (PP-InsPs), which are signalling molecules present in all eukaryotes and have been connected to P signalling in other organisms including plants, but their implications in other nutrient signalling are still under evaluation. In this study, we conducted prolonged starvation in WT and *vip1-1 Chlamydomonas* cells. After N and P had been consumed, they showed important differences in the levels of chlorophyll, photosystem II (PSII) activity and ultrastructural morphology, including differences in the cell size and cell division. Metabolomic analysis under these conditions revealed an overall decrease in different organic compounds such as amino acids, including arginine and its precursors and tryptophan, which is considered a signalling molecule itself in plants. In addition, we observed significant differences in RNA levels of genes related to N assimilation that are under the control of the NIT2 transcription factor. These data are of important relevance in understanding the signalling role of PP-InsPs in nutrient sensing, especially regarding N, which has not directly been connected to these molecules in green organisms before. Additionally, the PP-InsPs regulation over cell size and photosynthesis supports novel strategies for the generation of resilient strains, expanding the biotechnological applications of green microalgae.

1 | INTRODUCTION

In recent years, environmental challenges derived from uncontrolled CO_2 emissions and other contamination sources have become a global priority. Improving water management and combating climate change have been included in the 2030 Agenda (https://sdgs.un.org/2030agenda) and the SDGs of the United Nations to transform our planet. Therefore, it is interesting to find sustainable solutions, including the use of green organisms to address these problems. In this context, the use of microalgae stands as an interesting solution to achieve a reduction in greenhouse gas emissions through CO_2 fixation in photobioreactors and sustainable wastewater treatment (Raeesossadati et al., 2014; Kaloudas, Pavlova and Penchovsky, 2021; Plöhn et al., 2021). Although we need to scale up and standardize the use of these microorganisms, we also need to understand the molecular mechanisms that make them adapt to environmental unfavourable conditions. In this way, *Chlamydomonas reinhardtii* is a single-celled green microalga that has been extensively used in different scientific

This is an open access article under the terms of the Creative Commons Attribution License, which permits use, distribution and reproduction in any medium, provided the original work is properly cited.
© 2025 The Author(s). *Physiologia Plantarum* published by John Wiley & Sons Ltd on behalf of Scandinavian Plant Physiology Society.

contexts due to its well-characterized genetics and easy cultivation (Merchant et al., 2007; Harris, 2009). It has served as a model organism for nutrient-deprivation responses, such as carbon limitation (Wang, Stessman and Spalding, 2015), phosphorous deprivation (Kamalanathan et al., 2016; Hidayati et al., 2019; Couso et al., 2020; Zúñiga-Burgos et al., 2024), sulfur deprivation (González-Ballester et al., 2010; De Mia et al., 2019; Kajikawa et al., 2019; Grechanik et al., 2020) and nitrogen deprivation (Miller et al., 2010; Schmollinger et al., 2014; Park et al., 2015; Saroussi, Wittkopp and Grossman, 2016; Calatrava et al., 2019). Indeed, nitrogen assimilation mechanisms discovered in *C. reinhardtii* helped to elucidate how these processes are regulated in plants (Camargo et al., 2007; Castaings et al., 2009). To date, many efforts have been made to achieve biotechnological viability in using microalgae with waste products as a nutrient source (Behl et al., 2020; Han, Zhang and Ho, 2023). However, in these applications, the nutrient input might fluctuate over time, leading to temporarily limited nutrient conditions, especially under prolonged cultivation. So, it is important to improve our knowledge regarding nutrient limitation responses in microalgae to achieve optimal conditions in these biotechnological applications.

In *C. reinhardtii*, as well as in many other eukaryotic organisms, the Ser/Thr kinase Target of Rapamycin (TOR) is a conserved master regulator that integrates nutrient availability and energy levels to control central processes like amino acid, lipid and tetrapyrrole metabolism, nitrogen assimilation or carbon storage (Imamura et al., 2015; Kleessen et al., 2015; González and Hall, 2017; Mubeen et al., 2018; Roustan and Weckwerth, 2018; Pancha et al., 2020). In a previous study, the strain *vip1-1* was isolated in a rapamycin hypersensitivity screening of *C. reinhardtii* insertional mutants. This strain was deficient in highly phosphorylated inositol polyphosphate species, namely 1-diphosphoinositol 2,3,4,5,6-pentakisphosphate (1-PP-InsP_5), 5-diphosphoinositol 1,2,3,4,6-pentakisphosphate (5-PP-InsP_5) and 1,5-bis-diphosphoinositol 2,3,4,6-tetrakisphosphate (1,5-PP-InsP_4) (Couso et al., 2016). These molecules are synthesized through consecutive phosphorylation of the *myo*-inositol and are usually referred to as inositol pyrophosphates (PP-InsPs), as they contain at least one pyrophosphate in their structure (Shears, 2015; Williams, Gillaspy and Perera, 2015; Shears and Wang, 2020). The mutant strain *vip1-1* presents an insertion in the *vip1* gene, which encodes an inositol hexakisphosphate kinase responsible for the synthesis of inositol pyrophosphates in *C. reinhardtii* (Couso et al., 2016). PP-InsPs have been described as cell messengers which are involved in central signalling pathways mainly controlling protein phosphorylation, energy levels and P homeostasis in eukaryotic organisms including the green lineage (Saiardi, 2012; Nguyen Trung, Furkert and Fiedler, 2022; Pipercevic et al., 2023; Wu et al., 2023; Mihiret, Schaaf and Kamleitner, 2024). Interestingly, synergistic signalling between TOR and PP-InsPs was described, uncovering the role of these molecules in carbon partitioning and tricarboxylic acid cycle control in *Chlamydomonas* (Couso et al., 2016). Moreover, a phosphoproteomic approximation using *vip1-1* strain revealed that the signalling network of the PP-InsPs exerts regulation over cellular energy levels and light stress response through regulation of non-photochemical quenching mechanisms in green algae (Couso et al., 2021). In the same work, it was also found that PP-InsPs affected the phosphorylation status of the photosynthetic apparatus, which leads to state transitions, further supporting the signalling role of these highly phosphorylated molecules in stress adaptations. Additionally, precursors of PP-InsPs have been shown to respond to CO_2 levels in *Chlorella sorokiniana* and *Chlorella vulgaris* (Morales-Pineda et al., 2023), which is an important finding to further explore the biotechnological applications of this biosynthetic pathway.

Altogether, these reports highlight the emerging role of inositol polyphosphates (InsPs), especially the PP-InsPs, in nutrient sensing and stress response. Therefore, we decided to study the regulation of PP-InsPs over nutrient limitation responses in *C. reinhardtii* in order to expand our knowledge in nutrient signalling, which can be potentially useful to find and optimize new strategies regarding the applicability of microalgae in carbon sequestration and wastewater treatment. To address this task, we employed general nutrient deficiency by performing batch cultivation over an extended period of time in WT and *vip1-1*, which allowed us to capture different nutrient deprivation responses. Our results indicate that PP-InsPs regulate chlorophyll turnover and photosynthetic capacity under nutrient limitation. Under the same conditions, TEM analysis revealed differences in the ultrastructure of the PP-InsPs defective cells, including starch accumulation, the level of vacuolization and aberrant control of cell division. Moreover, we found that the metabolic profile of *Chlamydomonas* is deeply affected by the depletion of PP-InsPs in nutrient-stressed cells, resulting in a remarked reduction in amino acid levels. Additionally, the transcriptomic data showed that these molecules are required for the nitrogen deprivation response controlled by the transcription factor NIT2. Therefore, this study provides new insights into the multi-layered regulatory effects of PP-InsPs regarding nutrient management and presents their biosynthetic pathway as a potential genetic engineering target for biotechnological applications of green organisms.

2 | MATERIALS AND METHODS

2.1 | Strains and culture conditions

Chlamydomonas reinhardtii strain CC-1690 wild-type MT+ (Sager 21gr) (WT) (Sager, 1955) was used as the control strain, while the insertional mutant of the CC-1690 strain named *vip1-1* (Couso et al., 2016) was used as the object of study. The algal strains were grown at 25°C under 50 μmol m^{-2} s^{-1} photon flux density provided by OSRAM LED lamps. The experiments were initiated during the exponential growth phase (1–2 × 10^6 cells mL^{-1}) in liquid TAP (tris acetate phosphate) medium, and performed after 24 hours (control), 14 or 21 days (nutritional stress) as stated for each experiment.

2.2 | Dry cell weight, number of cells and nutrient availability in the media

Dry cell weight (DCW) was determined by filtering an exact volume of microalgae culture (3 mL) on pre-targeted glass-fibre filters

(0.45 μm pore size). The filter was washed with 3 mL solution of ammonium formate (0.5 M) to remove salts and dried at 80°C for 24 h. The dried filters were weighed in an analytical balance, and the dry weight was calculated by difference.

The cell number determinations were performed using a Neubauer chamber (Depth 0.2 mm, Fuchs-Rosenthal, Marienfeld). To prepare the hemocytometer, 10 μL of the cell suspension was used. The counting chamber was then placed on a microscope (Olympus CX23), and the counting was performed using a 40× objective lens. Large square regions at each corner of the grids on the hemocytometer were used for the cell counting.

Nutrient levels were determined after 24 h, 14 days and 21 days of batch culture. The culture was centrifuged to separate cells from the medium. Phosphate concentration was determined using the method described by Chen et al. (1956) and Christianson and Dunham (2005). Ammonium concentration was determined using the Nessler method, as reported by Eaton et al. (2005).

2.3 | Transmission electron microscopy

Cultures were collected at 1-2×10^6 cells mL^{-1} and fixed with 2.5% glutaraldehyde in 0.1 M Na-cacodylate buffer at pH 7.4 for 2 h at room temperature. After fixation, cells were washed three times with the same buffer at room temperature. Samples were post-fixed in 1% osmium tetraoxide in cacodylate buffer (0.1 M, pH 7.4) for 1 h at 4°C. After washing, samples were immersed in 2% uranyl acetate, dehydrated through a gradient acetone series (50, 70, 90, and 100%), and embedded in Spurr resin (Spurr, 1969). Semi-thin 147 sections (300 nm thickness) were obtained with a glass knife and stained with 1% toluidine blue for cell localization and reorientation using a conventional optic microscope. Once a suitable block face of the selected area was trimmed, several ultrathin sections (70 nm) were obtained using an ultramicrotome (Leica UC7) equipped with a diamond knife (Diatome) and collected on 200 mesh copper grids. Sections were examined in a Zeiss Libra 120 transmission electron microscope and digitized (2048 × 2048 × 16 bits) using an on-axis mounted TRS camera. WinTEM™ was used to analyze images.

2.4 | RNA-seq data generation and processing

Three independent biological replicates were considered for each strain and condition: WT strain after 24 h (control) and 14 days of growth (nutritional stress), and *vip1-1* strain after 24 h (control) and 14 days of growth (nutritional stress). RNA extraction was performed using mechanical disruption of the frozen cell pellets in a Mini Bead Beater (Biospe Products) mixed with 0.5 mm glass beads for individual cell lysis in the presence of an extraction buffer consisting of phenol:chloroform (1:1, v/v). RNA was purified using the ISOLATE II RNA Plant Kit (Bioline) following the manufacturer's instructions. The quality of the RNA was first analyzed by gel electrophoresis, and the RNA integrity number (RIN) was computed using Agilent 2100 Bioanalyzer. RNA-seq data generation was obtained as described in Serrano-Pérez et al. (2022), and analyzed using the MARACAS tool (Romero-Losada et al., 2022). Approximately 30 million 50 nt reads were obtained per sample. The RNA-Seq data was processed using fastQC (https://www.bioinformatics.babraham.ac.uk/projects/fastqc/) to perform the quality control, Hisat2 (Kim et al., 2019) to map reads, Stringtie (Pertea et al., 2015) to assemble the transcripts and Ballgown (Frazee et al., 2015) to quantify expression. Raw data was normalized using the upper quantile method, and low-accumulated genes (FPKM <0.5 in all conditions) were pre-filtered. Differential expression analysis was performed using the Limma R package (Ritchie et al., 2015), based on linear models, and the DESeq2 R package (Love, Huber and Anders, 2014), which relies on a negative binomial distribution. The minimum fold-change was set to 2, and the minimum adjusted *p*-value to 0.05 (the BH method was used to adjust *p*-values). In histograms of gene expression, the values are displayed in Fragments Per Kilobase of transcript per Million mapped reads (FPKM) after quantile normalization.

2.5 | Metabolomic data generation and processing

Five independent biological replicates were assessed for each strain and condition: WT strain after 24 h (control) and 14 days of growth (nutritional stress), and *vip1-1* strain after 24 hours (control) and 14 days of growth (nutritional stress). The metabolite content determination was performed using cell pellets that firstly were lyophilized (Skadi-Europe TFD 8503), and stored at −20°C as described in Serrano-Pérez et al. (2022). Metabolites were determined from 15–20 mg of lyophilized cell biomass subjected to mechanical disruption in a Mini Bead Beater (Biospe Products) with 0.5 mm glass beads in the presence of 1 mL extraction buffer consisting of chloroform:methanol (3:7, v/v). Centrifugation at 5000 *g* for 5 min at RT was then performed and these two steps were repeated until the pellets were colorless. Supernatants were concentrated using a speed-vacuum (Eppendorf concentrator Plus), and then samples were resuspended using 200 μL of MiliQ water and submitted to UPLC/MS analysis as described in Mccloskey and Ubhi (2015). Raw data was normalized using 10 μM paracetamol as an internal standard and the dry weight of each sample. The significance was calculated using the Wilcoxon signed-rank test, using the "stats" R package (https://www.R-project.org/), and the p-values obtained were adjusted using the Benjamini-Hochberg method implemented in the "qvalue" R package (Storey, 2011). Individual metabolite graphics were obtained using ggplot2 R package (Wickham, 2016), while the heatmap was generated using MetaboAnalyst 6.0 web tool (Pang et al., 2024) after auto-scaling each metabolite. Hierarchical clustering of metabolites was performed using Ward's method and Euclidean distance to group metabolites behaving similarly across different samples.

2.6 | Chlorophyll determination and activity assays

Two independent biological replicates and two technical replicates were used for chlorophyll determination and activity assays in all conditions tested. 1-2×10^6 cells mL^{-1} cultures of WT and *vip1-1* were used as controls. Chlorophyll determination was performed collecting

cells by centrifugation at 6500 *g*, resuspended in methanol and incubated at 70°C for 15 min. The supernatant obtained was then centrifugated at 6500 *g* and used to perform OD determination using a Thermo Scientific Genesys 30 spectrophotometer. The concentration of chlorophyll in the different samples was then calculated by measuring the absorbance at 650 and 665 nm, according to Mackinney (1941).

The enzymatic activity of nitrate reductase was calculated in the different samples according to Paneque et al. (1965) with slight modifications. Cells were permeabilized by shaking vigorously for 10 s with 20 µL of toluene per mL of culture. 0.2 mL of a 0.5 M Tris–HCl and 50 mM KNO_3 solution was added to 0.2 mL of cell culture, together with 0.2 mL of 1 mM FMN and water to a 0.9 mL final volume. 0.1 mL of a solution containing 8 mg mL^{-1} of $Na_2S_2O_4$ in 95 mM $NaHCO_3$ was added to the preparation to start the reaction, and after shaking, the samples were incubated for 10 min at 30°C. The reaction was stopped with 1 mL of a sulfanilamide preparation (10 g L^{-1} sulfanilamide, 200 mL HCl 37% v/v, and water to 1 L), 1 mL of N-(1-Naphthyl) ethylenediamine dihydrochloride at 200 mg L^{-1} and 2 mL of miliQ water. After 10 min at room temperature, absorbance is determined at 540 nm. The enzymatic activity of glutamine synthetase was calculated in the same conditions, according to Shapiro and Stadtman (1970). Activity is displayed in mU, which corresponds to the amount of enzyme necessary to catalyze one nanomole of substrate per minute.

2.7 | Chlorophyll fluorescence measurements

Batch cultures of WT and *vip1-1* cells were grown in control conditions and 21 days in TAP medium at 25°C. We used cell suspensions of 2×10^6 cells mL^{-1} and the measurements were performed in triplicate. Chlorophyll *a* fluorescence was measured using a pulse-amplitude modulation fluorometer (DUAL-PAM-100, Walz). The maximum quantum yield of PSII was assayed after incubation of the cell suspension in the dark for 20 min with constant stirring by calculating the ratio of the variable fluorescence, Fv, to maximal fluorescence, Fm, (Fv/Fm). The induction/recovery curve was performed by exposing dark-adapted samples to constant illumination at 50 µmol m^{-2} s^{-1} light intensity for 7 min, followed by 6 min of darkness. Effective PSII quantum yield (Y(II)) was determined using saturating pulses of red light at 5000 µmol m^{-2} s^{-1} intensity and 100 ms duration. Y(II) was then calculated by the DUAL-PAM-100 software according to the equations reported by Kramer et al. (2004). Error bars indicate the standard deviation (SD) of the values obtained from experiments performed in triplicate.

3 | RESULTS

3.1 | Inositol pyrophosphates affect chlorophyll accumulation under nutritional stress

The *Chlamydomonas reinhardtii* insertional mutant *vip1-1* was characterized by Couso and colleagues and described as a strain deficient in pyrophosphorylated inositol species ($InsP_7$ and $InsP_8$) (Couso et al., 2016). This mutant showed a very interesting phenotype when subjected to long limiting nutritional conditions (or nutritional stress, NS) under batch culturing, acquiring a greener appearance than WT despite displaying no differences in control conditions (Figure 1A). Accordingly, chlorophyll quantification revealed that the mutant strain had similar levels of these pigments compared to the WT in control conditions but increased 45% their chlorophyll content when subjected to nutritional stress after 21 days of batch cultivation (Figure 1B). Chlorophylls interact with different light-harvesting complexes to allow light absorption and structural stabilization in the photosynthetic apparatus (Bujaldon et al., 2017; Wang and Grimm, 2021). Therefore, we proceeded to assess the quantum yield of the photosystem II of the WT and mutant strains under control conditions and nutritional stress. We also evaluated the degree of damage at PSII by performing induction/recovery curves in the same conditions and strains (Figure 1C and D). We found that PSII activity was moderately affected in the *vip1-1* strain under control conditions, suggesting PP-InsPs are important to maintain optimal photosynthetic activity. Additionally, under nutritional limiting conditions, the maximum quantum yield of PSII (Y(II)) from the *vip1-1* mutant strain was further reduced to 55% compared to WT (Figure 1C). Although Y(II) was affected in both strains after nutrient limitation, induction/recovery curves (Figure 1D) showed a better recovery of PSII in WT than *vip1-1*, suggesting an important downregulation of the photosynthetic capacity of this mutant under these conditions. All these data indicate that PP-InsPs regulate the coupling of chlorophyll degradation and photosynthetic performance of the algal cells under nutrient limitation, which seems to have an important role in the adaptation to nutritional stress conditions for green microalgae.

3.2 | PP-InsPs influence ultrastructural adaptations to nutrient limitation

The increase in chlorophyll content together with limited Y(II) in a PP-InsPs deficient mutant under nutritional stress conditions (Figure 1B, C) may indicate that the *vip1-1* strain might show substantial differences at the ultrastructural level. We analyzed transmission electron microscopy (TEM) images from WT and *vip1-1* strains under control conditions (Figure 2A, D, G, J), 14 days (Figure 2B, E, H, K) and 21 days (Figure 2C, F, I, L) of batch cultivation. These conditions mimic a complete nutritional limitation that not only depends on one major element. In this regard, we measured the amount of ammonium and phosphate left in the medium under control conditions, 14 and 21 days and corroborated that these nutrients were fully consumed (Supplementary Figure 1A, B). After the TEM image analysis, we found important structural differences in *vip1-1* cells compared to WT that became more evident as the nutritional limitation was longer. We observed major differences between WT and *vip1-1* cells in the number of vacuoles and the electrodense material inside them under the control conditions (Figure 2; WT panels A and D; *vip1-1* panels G and J). TEM sections containing *vip1-1* cells held between 10–12 vacuoles, while we could only observe 3–4 vacuoles in WT cells under control conditions. After 14 and 21 days, the number of vacuoles in both

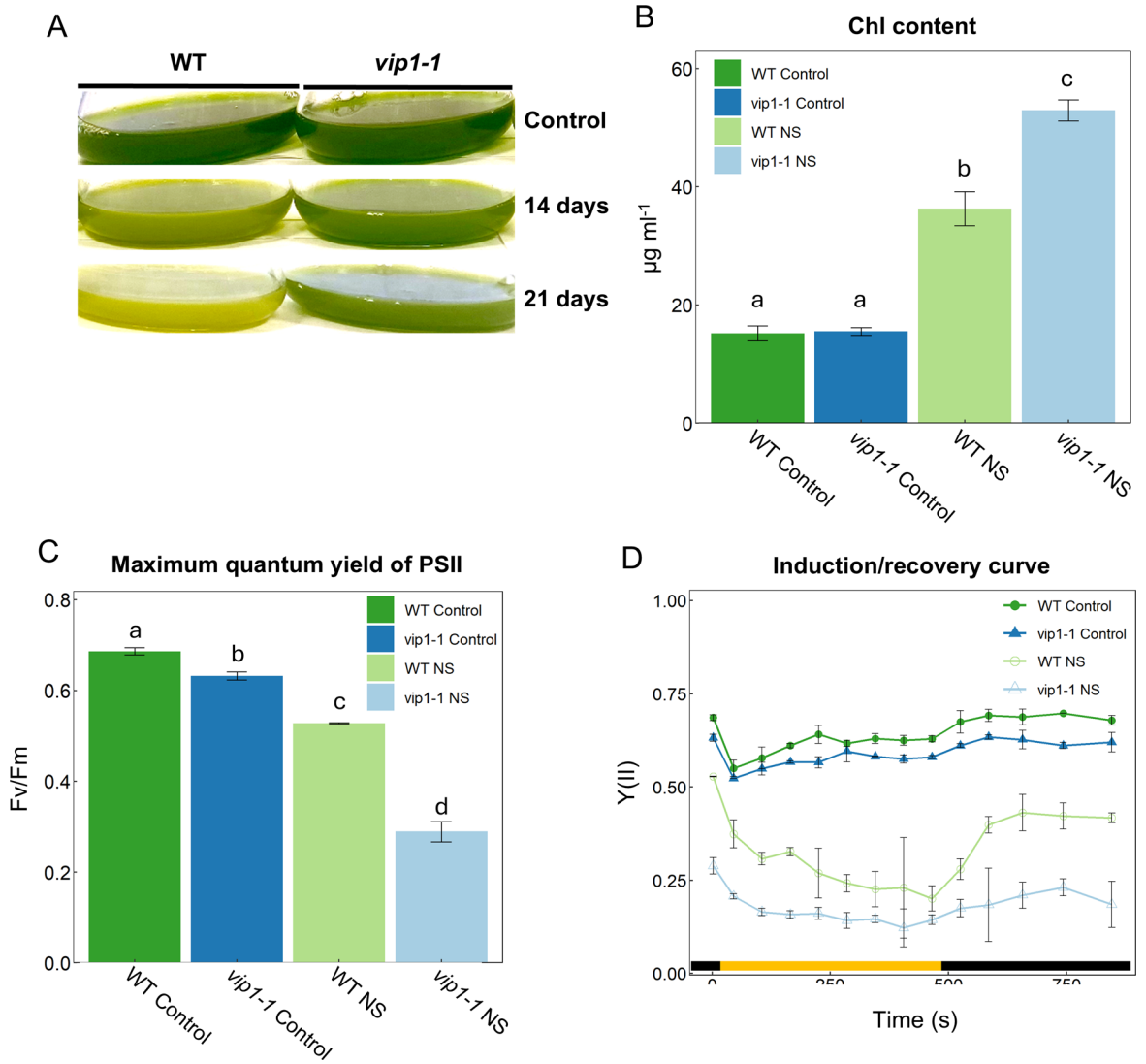


FIGURE 1 Appearance of cultures (A) after 24 hours (control), 14 and 21 days of batch cultivation (nutritional stress, NS). B and C, chlorophyll content (B) and maximum quantum yield of photosystem II (C) of WT and *vip1-1* strains after 24 hours (control) and 21 days of batch cultivation. D, Induction / recovery curve under control and NS conditions in WT and *vip1-1*, where the light exposure is represented with a yellow band. Significant differences are represented with different letters, evaluated using the Wilcoxon signed-rank test for B and Student's t-test for C. Error bars indicate mean ± SD.

strains were very similar. TEM analysis also showed some rounded structures inside vacuoles under control conditions (Figure 2G, J) that could reflect a higher autophagic activity of *vip1-1*. This was described in Heredia-Martínez et al. (2018) in WT cells treated with cerulenin. These bodies are usually produced by the autophagic process under stress conditions, suggesting that PP-InsPs are involved in the regulation of autophagy together or in combination with TOR, as we previously reported in Couso et al. (2021). Moreover, we found differences between WT and *vip1-1* strains in the number and size of starch granules, as *vip1-1* cells started with fewer and smaller starch granules than WT under control conditions (Figure 2A, D, G, J). However, after nutritional stress, starch granules were very similar in number in both algal strains (Figure 2C, F, I, L). These observations were confirmed by the analytical determination of starch (Supplementary Figure 1C), which shows an important increase in the starch levels in both algal strains after 21 days.

Additionally, when we analyzed *C. reinhardtii* cells after 21 days of nutrient limitation, we found that *vip1-1* cells were shrunk. This was confirmed after measuring the number of cells per gram of DCW (Supplementary Figure 2B), which revealed that *vip1-1* cells were significantly smaller (32% smaller) as observed in TEM analysis (Figure 2C, F, I, L; Supplementary Figure 2A). In these conditions, *vip1-1* cells exhibited several plasmatic membranes while WT cells did not (Figure 2C, F, I, L; Supplementary Figure 2A). These data are likely suggesting defects in the control of commitment size (Liu et al., 2023) to perform division in *vip1-1* cells that result in non-fully divided cells that end up accumulating plasmatic membranes (Figure 2I, L; Supplementary Figure 2A, bottom panels).

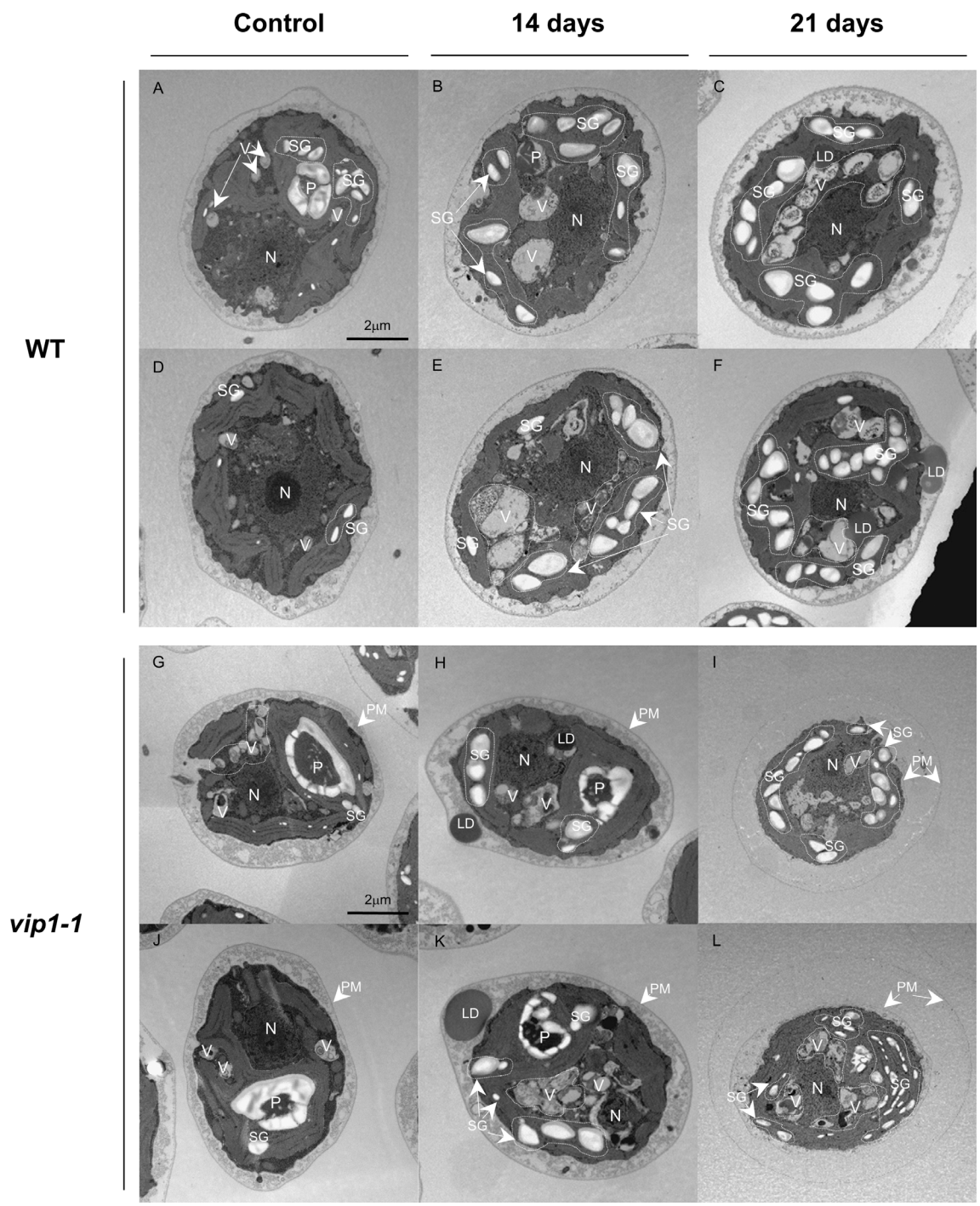


FIGURE 2 Transmission Electron microscopy (TEM) images from WT (top panels, A to F) and *vip1-1* (bottom panels, G to L). Images from WT (A, D) and *vip1-1* (G, J) correspond to cells under control conditions. Images from WT (B, E) and *vip1-1* (H, K) correspond to cells after 14 days in batch cultivation. Images from WT (C, F) and *vip1-1* (I, L) correspond to cells after 21 days in batch cultivation. (V), vacuoles; (P), pyrenoid; (N), nucleus; (PM), plasma membrane; (SG), starch granules; (LD), lipid droplets.

3.3 | Metabolomic analysis reveals effect of PP-InsP in N assimilation

In order to detect possible differences and deregulations in metabolic routes in *vip1-1* under nutritional limitation (NS), we performed a metabolomic analysis of the WT and *vip1-1* strains under control and prolonged cultivation conditions. UPLC/MS was used (see methods section) to analyze over 50 metabolites belonging to different metabolic pathways. Changes in metabolite accumulation were captured using a heatmap plot (Figure 3A) generated by MetaboAnalyst 6.0 (Pang et al., 2024). A widespread decrease in metabolite content as a response to nutritional stress became evident for both the WT and

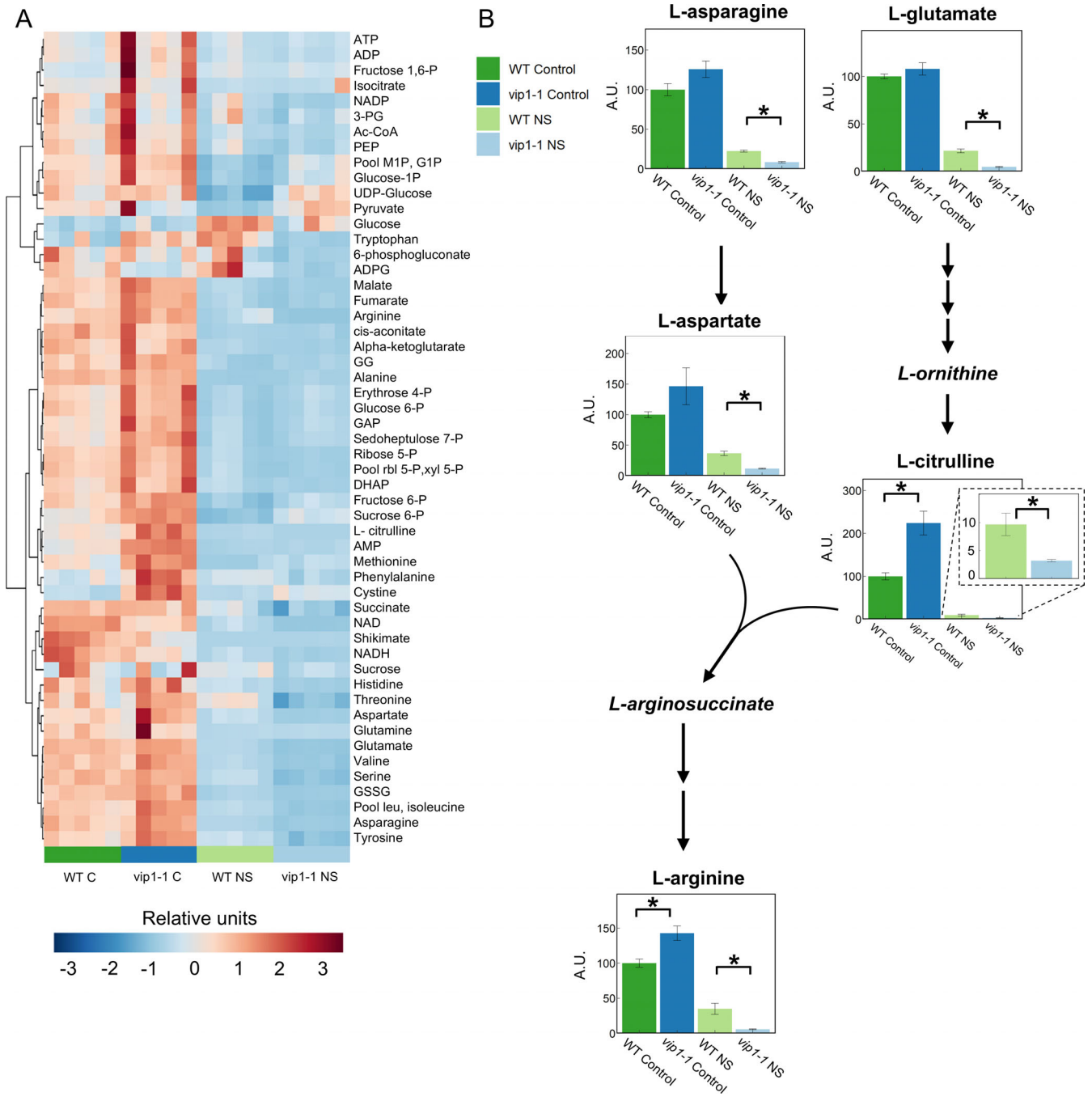


FIGURE 3 Heatmap of metabolites (A) representing their levels in each biological sample treated under control conditions (C) and nutrient starvation (NS). Row clustering was calculated using Ward's method and euclidean distance. B, diagram of the arginine biosynthetic pathway and the accumulation levels of some intermediates, relative to WT control levels. Consecutive arrows represent omitted intermediates, cursive letters indicate non-determined metabolites. Asterisks represent significant differences (adjusted p-value <0.05), evaluated using Wilcoxon rank-sum test with the BH procedure adjustment. Error bars indicate mean ± SE.

the *vip1-1* strains. Remarkably, we noticed that the absence of PP-InsPs produced a strong effect on the amino acid contents. In control conditions, *vip1-1* showed significantly higher levels of arginine, cystine, methionine, tyrosine, phenylalanine histidine, tryptophan and L-citrulline (Supplementary Table I). When the cells were subjected to nutrient limitation, 12 and 2 amino acids were significantly downregulated and upregulated, respectively, in the *vip1-1* strain (Supplementary Table I). This general increase in nutrient-replete conditions and decrease in nutrient limitation suggests that the absence of PP-InsPs prevents the *vip1-1* strain from correctly adjusting to the metabolic demands. Tryptophan, arginine and L-citrulline stood out because they were highly accumulated in *vip1-1* under control conditions but greatly reduced in nutrient stress conditions (approximately between 3- to 6-fold reduction) (Figure 3A; Table SI). However, tryptophan functions as a regulatory compound to

coordinate growth and stress responses in plants (Liu et al., 2022), little is known about its effect on microalgae besides translation. On the other hand, in *C. reinhardtii*, the arginine biosynthetic pathway has been proposed to participate in responses to the nitrogen status. High arginine levels, through the production of nitric oxide and possibly other signalling pathways, lead to the repression of nitrogen assimilatory mechanisms such as nitrate transporters and nitrate reductase (de Montaigu et al., 2010; González-Ballester et al., 2018; Monteiro, Giraldi and Winck, 2023). Interestingly, we detected at least a 2.5-fold reduction in the metabolites involved in the arginine biosynthesis, including the intermediate L-citrulline in the *vip1-1* mutant compared to the WT strain under nutritional stress conditions (Supplementary Table I, Figure 3B).

Additionally, pyruvate, glucose-1P, and UDP-glucose were grouped together using the clustering algorithm. They did not show differences under control conditions between strains but were significantly more abundant under nutritional stress in the *vip1-1* mutant strain (Supplementary Table I). These compounds take part in central carbon biosynthetic pathways, like amino acid and tricarboxylic acid cycle intermediates (pyruvate), starch (glucose-1P) or glycerolipids (UDP-glucose) (Deschamps, Ball and Dauvillée, 2023; Li-Beisson et al., 2023; Zhu et al., 2024). However, the glucose-1P must be transformed into ADP-glucose in order to synthesize starch out of glucose-1P, and we observed a significant 8-fold reduction in ADP-glucose accumulation in the *vip1-1* strain compared to the WT under nutritional deficiency (Supplementary Table I). In these conditions, we also found a significant decrease in starch levels in *vip1-1* compared to the WT in control conditions, but these differences were alleviated after 21 days (Supplementary Figure 1C).

These results suggest a role for inositol pyrophosphates in the sensing of nutrient availability, particularly nitrogen, together with carbon utilization, possibly through the fine-tuning of the signalling processes that govern the adaptations of the central carbon metabolism. However, the mechanism by which the PP-InsPs tune these signalling processes is still unclear, as both upregulation and downregulation of metabolites have been identified.

3.4 | PP-InsPs participate in N deprivation response through a multilayered regulation

The metabolic profiling of the PP-InsPs deficient strain *vip1-1* under nutritional stress (NS) revealed a reduction in amino acids involved in the biosynthesis of arginine, and arginine itself. Previously, arginine levels have been proposed to control transcription levels of N assimilation-related genes (González-Ballester et al., 2018; Monteiro, Giraldi and Winck, 2023). Therefore, we hypothesized that the PP-InsPs could be interfering with the transcriptomic response to nutrient limitation. In this context, we conducted an RNA-seq analysis of WT and *vip1-1* cultures under control and nutrient limitation. In *C. reinhardtii*, the N assimilation involves a complex regulatory network comprising ammonium and nitrate sensors, which induce transcription of the required genes, such as membrane transporters and reductase enzymes (Calatrava et al., 2023). Nitrate is incorporated into the cells through the NRT2 transporters that require the accessory protein NAR2, to be later reduced by the nitrate reductase NIT1/NIA1 and nitrite reductase NII1 to produce ammonium, while ammonium uptake is achieved through AMT1 transporters. We used ammonium in our culture medium as the N source, which resulted in no significant differences in the expression of nitrate assimilation-related genes between strains at control conditions (Figure 4A). However, when nutrient-limiting conditions were reached, we found that genes necessary for nitrate uptake and nitrate reduction lacked their activation response in the *vip1-1* cells as they do in WT under the same conditions (Figure 4A). In fact, *vip1-1* slows its growth under nitrate as a source of N compared to WT (Supplementary Figure 3). Even though we used general nutrient limitation conditions, *vip1-1* cells seem to display impairments in nitrogen depletion responses specifically. Current knowledge of nitrogen scavenging response in *C. reinhardtii* points to an upregulation in several genes (Schmollinger et al., 2014; Park et al., 2015). We found no significant differences between WT and *vip1-1* in the mRNA levels of different genes related to this process: ammonium transporters *amt1.2*, *amt1.5* and *amt1.8*, bispecific nitrate/nitrite transporters *nar1.2*, *nar1.6*, *nrt1.1*, and *nrt2.6*, glutamine synthetases *gln1*, *gln2*, *gln3* and *gln4* and glutamine oxoglutarate aminotransferases *gsn* and *gsf* (Supplementary Table II). In fact, glutamine synthetase (GS) activity was also measured under control conditions, and nutritional deficiency was observed in both strains (Supplementary Figure 4). Under control conditions, GS activity was very similar in both strains; however, after prolonged cultivation, GS activity was significantly higher in *vip1-1* compared to WT. This result points to an aberrant regulation of nitrogen scavenging that we further investigated. In this sense, we found genes lacking their activation response in nutrient deficiency in the *vip1-1* strain (*nrt2.1*, *nrt2.2*, *nar2*, *nit1* and *nii1*) (Figure 4A). These are all genes regulated by the transcription factor NIT2. Although no post-translational regulation has been reported on *nit2*, it is already known that the zinc finger protein NZF1 controls its expression, modifying the 3'UTR length of the *nit2* transcript (Higuera, Fernandez and Galvan, 2014; Sakuraba, Zhuo and Yanagisawa, 2022). We did not find significant differences in the mRNA accumulation levels of *nzf1 or nit2* genes (Supplementary Table II), which suggests that PP-InsPs might be either acting together with the NZF1 protein controlling *nit2* at the translational level or after *nit2* translation, mediating NIT2 activity as a transcription factor. In order to validate these findings, the activity of the nitrate reductase was assayed in the WT and *vip1-1* strains under control and nutrient deficiency conditions (Figure 4B). The results showed a significant reduction in the activity of this enzyme in the nutrient-limited *vip1-1* culture compared to the WT, which is consistent with the lack of mRNA accumulation of the nitrate reductase gene in *vip1-1* under these conditions (Figure 4B). Together, these results point to an important role of the PP-InsPs in nitrogen and possibly other nutrient limitations at the transcriptional level, facilitating the NIT2-driven transcriptomic response.

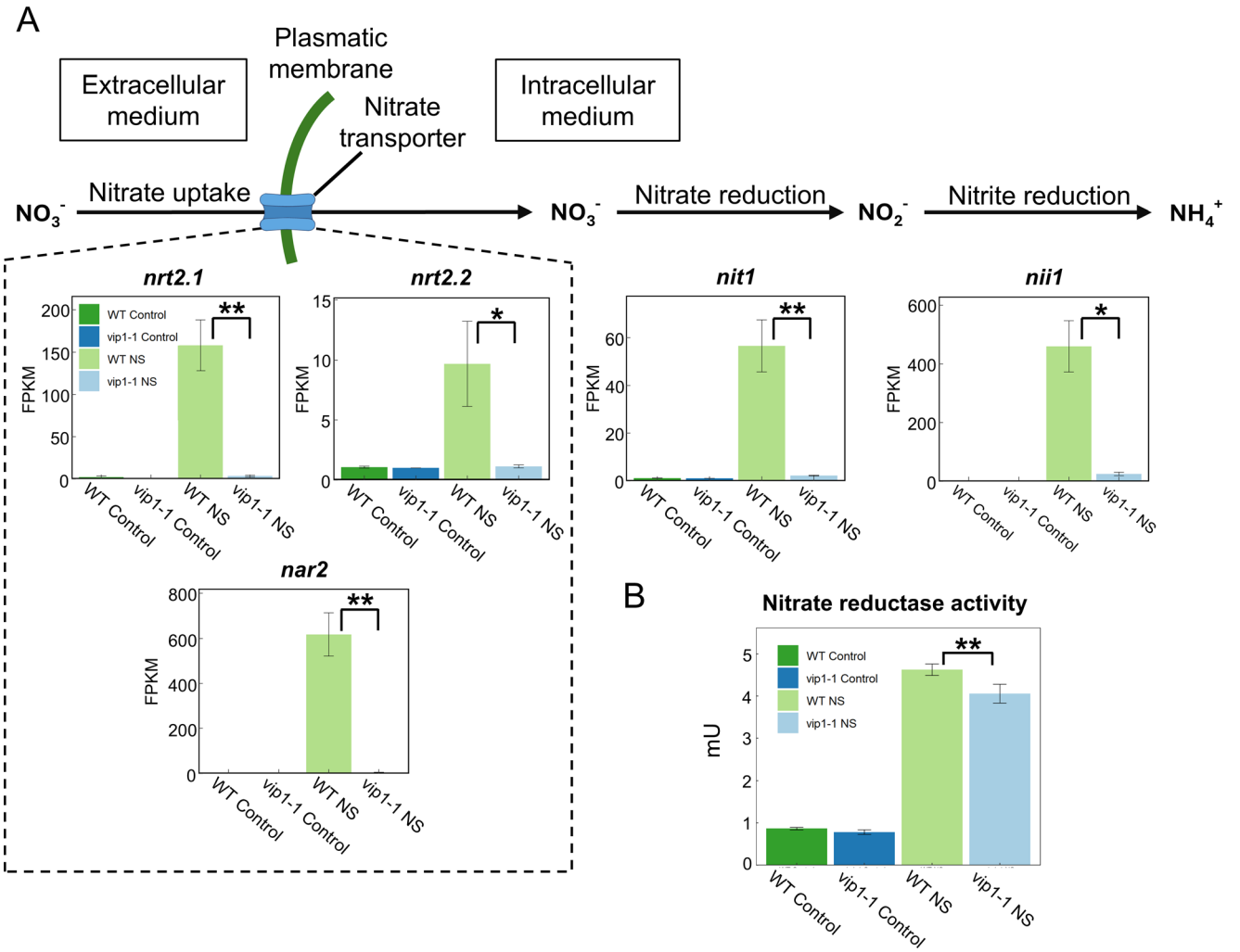


FIGURE 4 Diagram of nitrate assimilatory pathway (A), including gene expression of related genes. *nrt2.1* (Cre09.g410850) and *nrt2.2* (Cre09.g410800) encode nitrate transporters, both requiring the accessory protein encoded by *nar2* (Cre09.g410900). *nit1* (Cre09.g410950) encodes a nitrate reductase and *nii1* (Cre09.g410750) a nitrite reductase. Three independent biological replicates were analyzed in each condition (C; control and NS; nutritional stress) except from WT NS, where two independent biological replicates were analyzed. Error bars indicate mean ± SE. B, Nitrate reductase activity assay in each culture condition. Error bars indicate mean ± SD, asterisks indicate significant differences (* indicates $p < 0.05$, ** indicates $p < 0.01$).

4 | DISCUSSION

Prolonged cultivation causes nutrient limitation and stress in microalgal cultures, but these conditions are sometimes part of the scaling up process, which is fundamental for their biotechnological use. In fact, there are some microalgal strains that need to be grown on specific PBRs with medium uptake that have restrictive volumes and increase the cost of obtaining microalgal biomass (Wan Mahari et al., 2022). For this reason, it is important to understand which controlling mechanisms underlie the resilience of microalgal cultures under limited nutrient conditions. This study intended to understand the importance of PP-InsPs in nutrient limitation responses in the model single-cell microalga *Chlamydomonas reinhardtii*, using *vip1-1* mutant (Couso et al., 2016).

In this context, we found that the inositol pyrophosphates-deficient strain *vip1-1* displayed a very interesting phenotype with higher chlorophyll content than WT (Figure 1A and B) under nutritional deficiency (Supplementary Figure 1A, B). However, chlorophyll fluorescence measurements found less photosynthetic activity and an impaired recovery capacity in the mutant compared to WT cells, especially under nutritional deficiency after 21 days grown in batch (Figure 1C and D). In this sense, we previously reported aberrant regulation of autophagy in *vip1-1* (Couso et al., 2021) that could explain this difference. Chlorophagy has been previously reported in plants as an ATG-mediated process (Nakamura and Izumi, 2018; Jiang et al., 2020). The aberrant levels of ATG8 that we previously found in *vip1-1* after rapamycin treatment (Couso et al.; 2021) can indicate a slower/blocked process of autophagic degradation as described in Couso et al. (2018) that can end up in higher levels of chlorophylls in the mutant strain.

Alternatively, this phenotype has been shown by stay-green mutants in plants, in which mutations in genes involved in chlorophyll degradation were identified, leading to higher chlorophyll content and

reduced photosynthetic capacity (Cha et al. 2002; Balazadeh, 2014; Sakuraba et al. 2014). However, we did not find transcriptomic evidence regarding PP-InsPs affecting chlorophyll synthesis or breakdown, which hints that chlorophyll homeostasis must be affected by PP-InsPs in a post-transcriptional manner. In fact, we previously found important deregulation of the phosphorylation patterns of many proteins belonging to the PSII apparatus, including chlorophyll-binding proteins such as CP43 and CP47 and several proteins belonging to the light-harvesting antenna (Couso et al., 2021). Chlorophyll-binding proteins have been reported to have an important interconnection in the degradation of chlorophylls in leaf senescence (Hörtensteiner and Feller, 2002). This chlorophyll degradation is induced by senescence in plants but by nitrogen deprivation in microalgae like *C. reinhardtii*, although its regulation is yet to be elucidated (Chen et al., 2019; Willows, Lagarias and Duanmu, 2023). All these data indicate that PP-InsPs signaling is involved in the chlorophylls turnover by affecting the stability of the PSII. Also, the reduction in photosynthetic activity might be related to this chlorophyll accumulation affecting the structure and/or function of the photosynthetic apparatus or also to impairments in nitrogen scavenging mechanisms in *vip1-1*.

The chlorophyll-binding proteins account for 20% of the cellular nitrogen, and these proteins can only be recycled once chlorophylls have been released and degraded in plants (Wang and Grimm, 2021). Therefore, the observed chlorophyll accumulation in *vip1-1* (Figure 1A, B) suggests that inositol pyrophosphates are required for the nitrogen scavenging mechanisms related to chlorophyll and chlorophyll-binding protein recycling. In fact, the metabolic profiling revealed that amino acids involved in the arginine biosynthetic pathway were significantly reduced in the absence of inositol pyrophosphates only in nutrient deficiency conditions (Figure 3B). Arginine levels have been reported to participate in the signalling network responsible for post-transcriptional control in N-deprived *C. reinhardtii* cultures (Monteiro, Giraldi and Winck, 2023). Interestingly, the decrease shown by *vip1-1* in most amino acids during nutrient limitation, especially the arginine biosynthesis-related ones (arginine, asparagine, aspartate and glutamate), supports the reduced chlorophyll and chlorophyll-binding protein recycling discussed above.

Electrodense bodies inside vacuoles displayed by TEM images in the *vip1-1* cells were observed since the beginning of the experiment but were especially visible after 14 days (Figure 2H, K). This might be a consequence of the malfunctioning recycling process, which also correlates with lower amino acid accumulation under nutritional deficiency following deregulated intracellular nitrogen scavenging. In Couso et al. (2021), we reported aberrant ATG8 levels in *vip1-1* after rapamycin treatment that point to deregulation of autophagy in the mutant under nutritional stress conditions when TOR activity is highly reduced. Therefore, a compromised nutrient scavenging mechanism could explain the reduced cell size of the *vip1-1* cells when nutrient levels are strongly reduced, as shown in the TEM images and the number of cells per DCW (Figure 2C, F, I, L; Supplementary Figure 2A and B). However, the accumulation of plasma membrane in *vip1-1* cells after 21 days under cultivation (Figure 2I, L; Supplementary Figure 2A) suggests another explanation connected to cell cycle control. In *C. reinhardtii*, cells sense nutritional availability to either proceed with cell division or enter a quiescence state (Li, Umen and Jonikas, 2014; Cross and Umen, 2015; Takeuchi and Benning, 2019). This is evaluated during the G1 phase when a cell is committed to performing at least one S/M cycle if it grows past a certain size but arrests its cell cycle if growth has not surpassed this "commitment" point due to nutrient scarcity or other environmental factors (Cross and Umen, 2015). After mitosis, daughter cells remain inside the cell wall of the mother cell, and secretion of lytic enzymes is required to perform hatching (Kubo et al., 2009). The regulatory network where PP-InsPs take part might be interfering with the adequate cell cycle progression in *C. reinhardtii*, which has been previously described for the S phase in yeasts (Banfic et al., 2013). We think that the *vip1-1* cells are not able to correctly arrest their cell cycle, and they pass the "commitment" point with insufficient size (Liu et al., 2023). This could lead to faulty cell division and hatching process, thus explaining why we observe several plasmatic membranes surrounding the mutant cells after 21 days of batch culture as a result of aborted or incomplete mitosis events (Figure 2I, L; Supplementary Figure 2A, bottom panels).

Here, we also observed an impaired transcriptomic response involving transcriptional activation of key genes in nitrate scavenge, e.g., nitrate transporters *nrt2.1*, *nrt2.2*, *nar2*, nitrate reductase *nit1* and nitrite reductase *nii1*, which was confirmed with a nitrate reductase assay as an alternative analytical method (Figure 4A, B; Supplementary Table II). The transcriptomic response to nitrogen deprivation in *C. reinhardtii* involves several ammonium and nitrate transporters, as well as nitrate reductase, nitrite reductase and GS/GOGAT cycle enzymes (Schmollinger et al., 2014; Park et al., 2015). Nevertheless, only genes regulated by the transcription factor NIT2 were not activated under nutritional deficiency in the mutant, even though we did not find significant differences in *nit2* mRNA accumulation. The regulation of *nit2* is not well understood yet, although NZF1 activity has been reported to affect its mRNA 3'UTR length (Higuera, Fernandez and Galvan, 2014). Remarkably, this type of gene expression regulation has been found to be exerted by PP-InsPs in yeasts (Sanchez et al., 2019). These findings propose that these molecules must participate in nitrogen limitation responses controlling NIT2 activity, possibly modulating its 3'UTR length and signalling for intracellular nutrient recycling. Alternatively, PP-InsPs could regulate NIT2 activity through pyrophosphorylation, which is a post-translational modification (PTM) where a PP-InsP molecule is able to transfer its β-phosphoryl group to an already phosphorylated serine (Nguyen Trung, Furkert and Fiedler, 2022). Even though this PTM has only recently started to gain focus, it is known to occur on serine residues surrounded by glutamate and aspartate residues and located in a disordered region of the target protein (Chanduri and Bhandari, 2019; Ganguli et al., 2020; Mihiret, Schaaf and Kamleitner, 2024). Remarkably, the NIT2 protein (UniProt accession number A0A2K3DXI1) has several candidate serine residues in an acidic region. This is predicted to be a disordered region that is close to the RWP-RK domain in the C-terminal. This domain is present in different transcription factors that regulate the expression of genes

related to nitrogen utilization, gametogenesis and embryogenesis in plants and green algae (Camargo et al., 2007; Yin et al. 2020). Therefore, the pyrophosphorylation of one or some of these serine residues could be necessary for the activity of the NIT2 protein and possibly other transcription factors of the same family.

Additionally, the transcription factor NIT2 shares the RWP-RK domain with MID, which determines the mating type of *C. reinhardtii* cells and responds to N deficiency (Lin and Goodenough, 2007; Innami et al., 2022; Sakuraba, Zhuo and Yanagisawa, 2022). In this sense, the PP-InsPs might be necessary for the proper activity of MID in the same way that they are for NIT2, as previously discussed. Given these findings, the PP-InsPs could be integrating nitrogen deprivation responses and cell cycle control with nutrient availability, potentially through transcription regulation and possibly post-transcriptional regulation of transcription factors.

AUTHOR CONTRIBUTIONS

RBG, MEGG, and IC contributed to the planning and experimental design; RBG, MEGG, JMP and IC performed experiments and data analysis; and RBG, MEGG, JMP and IC wrote the manuscript.

ACKNOWLEDGEMENTS

RBG was also awarded as a FPU22/00688 fellow by Ministerio de Educación.

DATA AVAILABILITY STATEMENT

The raw and processed RNA-seq data that support the findings of this study are openly available in the Gene Expression Omnibus (https://www.ncbi.nlm.nih.gov/geo/) repository and can be accessed with the Identifier GSE276249. The raw RNA-seq data are openly available at the Sequence Read Archive (https://www.ncbi.nlm.nih.gov/sra) and can be accessed with the identifier PRJNA1156089. The raw and processed metabolomic data can be found in the MetaboLights repository (https://www.ebi.ac.uk/metabolights/) using the identifier MTBLS10779.

ORCID

Rodrigo Bedera-García https://orcid.org/0000-0001-7281-5020
José María Personat https://orcid.org/0000-0003-2273-5000
Inmaculada Couso https://orcid.org/0000-0003-2849-675X

REFERENCES

Balazadeh, S. (2014). Stay-green not always stays green. *Molecular Plant* 7, 1264–1266.

Banfic, H., Bedalov, A., York, J.D., Visnjic, D. (2013). Inositol pyrophosphates modulate S phase progression after pheromone-induced arrest in saccharomyces cerevisiae. *Journal of Biological Chemistry* 288, 1717–1725.

Behl, K., SeshaCharan, P., Joshi, M., Sharma, M., Mathur, A., Kareya, M.S., Jutur, P.P., Bhatnagar, A., Nigam, S. (2020). Multifaceted applications of isolated microalgae *Chlamydomonas* sp. TRC-1 in wastewater remediation, lipid production and bioelectricity generation. *Bioresource Technology*, 304.

Bujaldon, S., Kodama, N., Rappaport, F., Subramanyam, R., de Vitry, C., Takahashi, Y., Wollman, F.A. (2017). Functional Accumulation of Antenna Proteins in Chlorophyll b-Less Mutants of *Chlamydomonas reinhardtii*. *Molecular Plant*, 10, 115–130.

Calatrava, V., Hom, E.F.Y., Llamas, Á., Fernández, E., Galván, A. (2019). *Nitrogen scavenging from amino acids and peptides in the model alga* Chlamydomonas reinhardtii. The role of extracellular L-amino oxidase. Algal Research, 38.

Calatrava, V., Tejada-Jimenez, M., Sanz-Luque, E., Fernandez, E., Galvan, A. (2023). Nitrogen metabolism in *Chlamydomonas*. In: *The* Chlamydomonas *Sourcebook: Volume 2: Organellar and Metabolic Processes*. Elsevier, pp. 99–128.

Camargo, A., Llamas, Á., Schnell, R.A., Higuera, J.J., González-Ballester, D., Lefebvre, P.A., Fernández, E., Galván, A. (2007). Nitrate signaling by the regulatory gene NIT2 in *Chlamydomonas*. *Plant Cell*, 19, 3491–3503.

Castaings, L., Camargo, A., Pocholle, D., Gaudon, V., Texier, Y., Boutet-Mercey, S., Taconnat, L., Renou, J.P., Daniel-Vedele, F., Fernandez, E., Meyer, C., Krapp, A. (2009). The nodule inception-like protein 7 modulates nitrate sensing and metabolism in Arabidopsis. *Plant Journal*, 57, 426–435.

Cha, KW., Lee, YJ., Koh, HJ., Lee, BM., Nam, YW., Paek, NC. (2002). Isolation, characterization, and mapping of the stay green mutant in rice. *Theoretical and Applied Genetics*, 104, 526–532.

Chen, P.S., Toribara, T.Y., Warner, H. (1956). Microdetermination of Phosphorus. *Analytical Chemistry*, 28(11), 1756–1758.

Chen, Y., Shimoda, Y., Yokono, M., Ito, H., Tanaka, A. (2019). Mg-dechelatase is involved in the formation of photosystem II but not in chlorophyll degradation in *Chlamydomonas reinhardtii*. *Plant Journal*, 97, 1022–1031.

Christianson, C., Dunham, M. (2005). Modified Phosphate assay. *Dunham Lab Web*; http://dunham.gs.washington.edu/MDphosphateassay.htm. Accessed 28 Nov 2024

Couso, I., Evans, B.S., Li, J., Liu, Y., Ma, F., Diamond, S., Allen, D.K., Umen, J.G. (2016). Synergism between inositol polyphosphates and TOR kinase signaling in nutrient sensing, growth control, and lipid metabolism in *Chlamydomonas*. *Plant Cell*, 28, 2026–2042.

Couso, I., Pérez-Pérez, M.E., Martínez-Force, E., Kim, H.S., He, Y., Umen, J.G., Crespo, J.L. (2018). Autophagic flux is required for the synthesis of triacylglycerols and ribosomal protein turnover in *Chlamydomonas*. *Journal of Experimental Botany*, 69(6), 1355–1367.

Couso, I., Pérez-Pérez, M.E., Ford, M.M., Martínez-Force, E., Hicks, L.M., Umen, J.G., Crespo, J.L. (2020). Phosphorus Availability Regulates TORC1 Signaling via LST8 in *Chlamydomonas*. *Plant Cell*, 32, 69–80.

Couso, I., Smythers, A.L., Ford, M.M., Umen, J.G., Crespo, J.L., Hicks, L.M. (2021). Inositol polyphosphates and target of rapamycin kinase signalling govern photosystem II protein phosphorylation and photosynthetic function under light stress in *Chlamydomonas*. *New Phytologist*, 232, 2011–2025.

Cross, F.R., Umen, J.G. (2015). The *Chlamydomonas* cell cycle. *Plant Journal*, 82, 370–392.

De Mia, M., Lemaire, S.D., Choquet, Y., Wollmana, F.A. (2019). Nitric oxide remodels the photosynthetic apparatus upon S- starvation in *Chlamydomonas reinhardtii*. *Plant Physiology*, 179, 718–731.

de Montaigu, A., Sanz-Luque, E., Galván, A.G., Fernández, E. (2010). A soluble guanylate cyclase mediates negative signaling by ammonium on expression of nitrate reductase in *Chlamydomonas*. *Plant Cell*, 22, 1532–1548.

Deschamps, P., Ball, S.G., Dauvillée, D. (2023). The comparative, biochemistry, genetics, and evolution of starch metabolism in *Chlamydomonas reinhardtii*. In: *The* Chlamydomonas *Sourcebook: Volume 2: Organellar and Metabolic Processes*. Elsevier, pp. 23–50.

Eaton, AD. (2005). *Standard methods for the examination of water and wastewater*. 21st ed. American Public Health Association, Washington.

Frazee, A.C., Pertea, G., Jaffe, A.E., Langmead, B., Salzberg, S.L., Leek, J.T. (2015). Ballgown bridges the gap between transcriptome assembly and expression analysis. *Nature Biotechnology*, 33(3), 243–246.

Ganguli, S., Shah, A., Hamid, A., Singh, A., Palakurti, R., Bhandari, R. (2020). A high energy phosphate jump - From pyrophospho-inositol to pyrophospho-serine. *Advances in Biological Regulation*, 75.

González, A., Hall, M.N. (2017). Nutrient sensing and TOR signaling in yeast and mammals. *The EMBO Journal*, 36, 397–408.

González-Ballester, D., Casero, D., Cokus, S., Pellegrini, M., Merchant, S.S., Grossman, A.R. (2010). RNA-Seq analysis of sulfur-deprived *Chlamydomonas* cells reveals aspects of acclimation critical for cell survival. *Plant Cell*, 22, 2058–2084.

González-Ballester, D., Sanz-Luque, E., Galván, A., Fernández, E., de Montaigu, A. (2018). Arginine is a component of the ammonium-CYG56 signalling cascade that represses genes of the nitrogen assimilation pathway in *Chlamydomonas reinhardtii*. *PLoS One*, 13.

Grechanik, V., Romanova, A., Naydov, I., Tsygankov, A. (2020). Photoautotrophic cultures of *Chlamydomonas reinhardtii*: sulfur deficiency, anoxia, and hydrogen production. *Photosynthesis Research*, 143, 275–286.

Han, M., Zhang, C., Ho, S.H. (2023). Immobilized microalgal system: An achievable idea for upgrading current microalgal wastewater treatment. *Environmental Science and Ecotechnology*, 14.

Harris, E.H. (2009). *The* Chlamydomonas *sourcebook*, 2nd ed. Academic Press.

Heredia-Martínez, L.G., Andrés-Garrido, A., Martínez-Force, E., Pérez-Pérez, M.E., Crespo, J.L., 2018. Chloroplast damage induced by the inhibition of fatty acid synthesis triggers autophagy in *Chlamydomonas*. *Plant Physiology*, 178, 1112–1129.

Hidayati, N.A., Yamada-Oshima, Y., Iwai, M., Yamano, T., Kajikawa, M., Sakurai, N., Suda, K., Sesoko, K., Hori, K., Obayashi, T., Shimojima, M., Fukuzawa, H., Ohta, H. (2019). Lipid remodeling regulator 1 (LRL1) is differently involved in the phosphorus-depletion response from PSR1 in *Chlamydomonas reinhardtii*. *Plant Journal*, 100, 610–626.

Higuera, J.J., Fernandez, E., Galvan, A. (2014). *Chlamydomonas* NZF1, a tandem-repeated zinc finger factor involved in nitrate signalling by controlling the regulatory gene NIT2. *Plant, Cell and Environment*, 37, 2139–2150.

Hörtensteiner, S., Feller, U. (2002). Nitrogen metabolism and remobilization during senescence. *Journal of Experimental Botany*, 53, 927–937.

Imamura, S., Kawase, Y., Kobayashi, I., Sone, T., Era, A., Miyagishima, S. ya, Shimojima, M., Ohta, H., Tanaka, K. (2015). Target of rapamycin (TOR) plays a critical role in triacylglycerol accumulation in microalgae. *Plant Molecular Biology*, 89, 309–318.

Innami, R., Miyamura, S., Okoshi, M., Nagumo, T., Ichihara, K., Yamazaki, T., Kawano, S. (2022). *Gamete dimorphism of the isogamous green alga* (Chlamydomonas reinhardtii)*, is regulated by the mating type-determining gene*, MID. Communications Biology 5.

Jiang, Z., Zhu, L., Wang, Q., & Hou, X. (2020). Autophagy-Related 2 Regulates Chlorophyll Degradation under Abiotic Stress Conditions in Arabidopsis. *International Journal of Molecular Sciences*, 21(12), 4515.

Kajikawa, M., Yamauchi, M., Shinkawa, H., Tanaka, M., Hatano, K., Nishimura, Y., Kato, M., Fukuzawa, H. (2019). Isolation and Characterization of *Chlamydomonas* Autophagy-Related Mutants in Nutrient-Deficient Conditions. *Plant and Cell Physiology*, 60, 126–138.

Kaloudas, D., Pavlova, N., Penchovsky, R. (2021). Phycoremediation of wastewater by microalgae: a review. *Environmental Chemistry Letters*, 19, 2905–2920.

Kamalanathan, M., Pierangelini, M., Shearman, L.A., Gleadow, R., Beardall, J. (2016). Impacts of nitrogen and phosphorus starvation on the physiology of *Chlamydomonas reinhardtii*. *Journal of Applied Phycology*, 28, 1509–1520.

Kim, D., Paggi, J.M., Park, C., Bennett, C., Salzberg, S.L. (2019). Graph-based genome alignment and genotyping with HISAT2 and HISAT-genotype. *Nature Biotechnology* 37, 907–915.

Kleessen, S., Irgang, S., Klie, S., Giavalisco, P., Nikoloski, Z. (2015). Integration of transcriptomics and metabolomics data specifies the metabolic response of *Chlamydomonas* to rapamycin treatment. *Plant Journal*, 81, 822–835.

Kramer, D.M., Johnson, G., Kiirats, O., Edwards, G.E. (2004). New fluorescence parameters for the determination of Q A redox state and excitation energy fluxes, *Photosynthesis Research*, 79, 209–218.

Kubo, T., Kaida, S., Abe, J., Saito, T., Fukuzawa, H., Matsuda, Y. (2009). The *Chlamydomonas* hatching enzyme, sporangin, is expressed in specific phases of the cell cycle and is localized to the flagella of daughter cells within the sporangial cell wall. *Plant and Cell Physiology*, 50, 572–583.

Li, X., Umen, J.G., Jonikas, M.C. (2014). Waking sleeping algal cells. *Proceedings of the National Academy of Sciences of the United States of America*, 111(44), 15610–15611.

Li-Beisson, Y., Warakanont, J., Riekhof, W., Benning, C. (2023). *Chlamydomonas* glycerolipid metabolism. In: *The* Chlamydomonas *Sourcebook*: *Volume 2*: *Organellar and Metabolic Processes*. Elsevier, pp. 51–97.

Lin, H., Goodenough, U.W. (2007). Gametogenesis in the *Chlamydomonas reinhardtii* minus mating type is controlled by two genes, MID and MTD1. *Genetics*, 176, 913–925.

Liu, D., Vargas-García, C.A., Singh, A., Umen, J.G. (2023). A cell-based model for size control in the multiple fission alga *Chlamydomonas reinhardtii*. *Current Biology*, 33(23), 5215–5224.

Liu, W.C., Song, R.F., Zheng, S.Q., Li, T.T., Zhang, B.L., Gao, X., Lu, Y.T. (2022). Coordination of plant growth and abiotic stress responses by tryptophan synthase β subunit 1 through modulation of tryptophan and ABA homeostasis in Arabidopsis. *Molecular Plant*, 15, 973–990.

Love, M.I., Huber, W., Anders, S. (2014). Moderated estimation of fold change and dispersion for RNA-seq data with DESeq2. *Genome Biology*, 15.

Mackinney, G. (1941). Absorption of light by chlorophyll solutions. *Journal of Biological Chemistry*, 140, 315–322.

Mccloskey, D., Ubhi, B.K. (2015). *Quantitative and Qualitative Metabolomics for the Investigation of Intracellular Metabolism*. Framingham: SCIEX.

Merchant, S.S., Prochnik, S.E., Vallon, O., Harris, E.H., Karpowicz, S.J., Witman, G.B., Terry, A., Salamov, A., Fritz-Laylin, L.K., Maréchal-Drouard, L., Marshall, W.F., Qu, L.-H., Nelson, D.R., Sanderfoot, A.A., Spalding, M.H., Kapitonov, V. V, Ren, Q., Ferris, P., Lindquist, E., Shapiro, H., Lucas, S.M., Grimwood, J., Schmutz, J., Grigoriev, I. V, Rokhsar, D.S., Grossman, A.R. (2007). The *Chlamydomonas* Genome Reveals the Evolution of Key Animal and Plant Functions. *Science* 318, 245–250.

Mihiret, Y.E., Schaaf, G., Kamleitner, M. (2024). Protein pyrophosphorylation by inositol phosphates: a novel post-translational modification in plants? *Frontiers in Plant Science*, 15.

Miller, R., Wu, G., Deshpande, R.R., Vieler, A., Gartner, K., Li, X., Moellering, E.R., Zauner, S., Cornish, A.J., Liu, B., Bullard, B., Sears, B.B., Kuo, M.H., Hegg, E.L., Shachar-Hill, Y., Shiu, S.H., Benning, C. (2010). Changes in transcript abundance in *Chlamydomonas reinhardtii* following nitrogen deprivation predict diversion of metabolism. *Plant Physiology*, 154, 1737–1752.

Monteiro, L. de F.R., Giraldi, L.A., Winck, F.V. (2023). From Feasting to Fasting: The Arginine Pathway as a Metabolic Switch in Nitrogen-Deprived *Chlamydomonas reinhardtii*. *Cells*, 12.

Morales-Pineda, M., García-Gómez, M.E., Bedera-García, R., García-González, M., Couso, I. (2023). *CO2 Levels Modulate Carbon Utilization*, Energy Levels and Inositol Polyphosphate Profile in Chlorella. Plants, 12.

Mubeen, U., Jüppner, J., Alpers, J., Hincha, D.K., Giavalisco, P. (2018). Target of rapamycin inhibition in *Chlamydomonas reinhardtii* triggers

de novo amino acid synthesis by enhancing nitrogen assimilation. *Plant Cell*, 30, 2240–2254.

Nakamura, S., & Izumi, M. (2018). Chlorophagy is ATG gene-dependent microautophagy process. *Plant Signaling & Behavior*, 14(1).

Nguyen Trung, M., Furkert, D., Fiedler, D. (2022). Versatile signaling mechanisms of inositol pyrophosphates. *Current Opinion in Chemical Biology*, 70.

Pancha, I., Chokshi, K., Tanaka, K., Imamura, S. (2020). Microalgal Target of Rapamycin (TOR): A Central Regulatory Hub for Growth, Stress Response and Biomass Production. *Plant and Cell Physiology*, 61, 675–684.

Paneque, A., Del Campo, F.F., Ramirez, J.M., Losada, M. (1965). Flavin nucleotide nitrate reductase from spinach. *Biochimica et Biophysica Acta*, 109, 79–85.

Pang, Z., Lu, Y., Zhou, G., Hui, F., Xu, L., Viau, C., Spigelman, A.F., Macdonald, P.E., Wishart, D.S., Li, S., Xia, J. (2024). MetaboAnalyst 6.0: towards a unified platform for metabolomics data processing, analysis and interpretation. *Nucleic Acids Research*, 52, 398–406.

Park, J.J., Wang, H., Gargouri, M., Deshpande, R.R., Skepper, J.N., Holguin, F.O., Juergens, M.T., Shachar-Hill, Y., Hicks, L.M., Gang, D.R. (2015). The response of *Chlamydomonas reinhardtii* to nitrogen deprivation: A systems biology analysis. *Plant Journal*, 81, 611–624.

Pertea, M., Pertea, G.M., Antonescu, C.M., Chang, T.C., Mendell, J.T., Salzberg, S.L. (2015). StringTie enables improved reconstruction of a transcriptome from RNA-seq reads. *Nature Biotechnology*, 33, 290–295.

Pipercevic, J., Kohl, B., Gerasimaite, R., Comte-Miserez, V., Hostachy, S., Müntener, T., Agustoni, E., Jessen, H.J., Fiedler, D., Mayer, A., Hiller, S. (2023). Inositol pyrophosphates activate the vacuolar transport chaperone complex in yeast by disrupting a homotypic SPX domain interaction. *Nature Communications*, 14.

Plöhn, M., Spain, O., Sirin, S., Silva, M., Escudero-Oñate, C., Ferrando-Climent, L., Allahverdiyeva, Y., Funk, C. (2021). Wastewater treatment by microalgae. *Physiologia Plantarum*, 173, 568–578.

Raeesossadati, M.J., Ahmadzadeh, H., McHenry, M.P., Moheimani, N.R. (2014). CO2 bioremediation by microalgae in photobioreactors: Impacts of biomass and CO2 concentrations, light, and temperature. *Algal Research*, 6.

Ritchie, M.E., Phipson, B., Wu, D., Hu, Y., Law, C.W., Shi, W., Smyth, G.K. (2015). Limma powers differential expression analyses for RNA-sequencing and microarray studies. *Nucleic Acids Research*, 43.

Romero-Losada, A.B., Arvanitidou, C., de los Reyes, P., García-González, M., Romero-Campero, F.J. (2022). ALGAEFUN with MARACAS, microALGAE FUNctional enrichment tool for MicroAlgae RnA-seq and Chip-seq AnalysiS. *BMC Bioinformatics* 23.

Roustan, V., Weckwerth, W. (2018). Quantitative phosphoproteomic and system-level analysis of TOR inhibition unravel distinct organellar acclimation in *Chlamydomonas reinhardtii*. *Frontiers in Plant Science*, 871.

Sager, R. (1955). Inheritance in the Green Alga *Chlamydomonas* Reinhardi. *Genetics*, 40, 476–489.

Saiardi, A. (2012). How inositol pyrophosphates control cellular phosphate homeostasis? *Advances in Biological Regulation*, 52, 351–359.

Sakuraba, Y., Park, S.Y., Kima, Y.S., Wanga, S.H., Yood, S.C., Hörtensteiner, S., Paek, N.C. (2014). *Arabidopsis* STAY-GREEN2 Is a Negative Regulator of Chlorophyll Degradation during Leaf Senescence. *Molecular Plant* 7(8), 1288–1302.

Sakuraba, Y., Zhuo, M., Yanagisawa, S. (2022). RWP-RK domain-containing transcription factors in the Viridiplantae: biology and phylogenetic relationships. *Journal of Experimental Botany*, 13, 4323–4337.

Sanchez, A.M., Garg, A., Shuman, S., Schwer, B. (2019). Inositol pyrophosphates impact phosphate homeostasis via modulation of RNA 3′ processing and transcription termination. *Nucleic Acids Research*, 47, 8452–8469.

Saroussi, S.I., Wittkopp, T.M., Grossman, A.R. (2016). The Type II NADPH dehydrogenase facilitates cyclic electron flow, energy-dependent quenching, and chlororespiratory metabolism during acclimation of *Chlamydomonas reinhardtii* to nitrogen deprivation. *Plant Physiology*, 170, 1975–1988.

Schmollinger, S., Mühlhaus, T., Boyle, N.R., Blaby, I.K., Casero, D., Mettler, T., Moseley, J.L., Kropat, J., Sommer, F., Strenkert, D., Hemme, D., Pellegrini, M., Grossman, A.R., Stitt, M., Schroda, M., Merchant, S.S. (2014). Nitrogen-sparing mechanisms in *Chlamydomonas* affect the transcriptome, the proteome, and photosynthetic metabolism. *Plant Cell*, 26, 1410–1435.

Serrano-Pérez, E., Romero-Losada, A.B., Morales-Pineda, M., García-Gómez, M.E., Couso, I., García-González, M., Romero-Campero, F.J. (2022). Transcriptomic and Metabolomic Response to High Light in the Charophyte Alga Klebsormidium nitens. *Frontiers in Plant Science*, 13.

Shapiro, B.M., Stadtman, E.R. (1970). Glutamine synthetase (Escherichia coli). In: *Methods in Enzymology*, Methods in Enzymology. Academic Press, pp. 910–922.

Shears, S.B. (2015). Inositol pyrophosphates: Why so many phosphates? *Advances in Biological Regulation*, 57, 203–216.

Shears, S.B., Wang, H. (2020). Metabolism and functions of inositol pyrophosphates: Insights gained from the application of synthetic analogues. *Molecules*, 25.

Spurr, A.R., (1969). A Low-Viscosity Epoxy Resin Embedding Medium for Electron Microscopy *J. Ultrastructure Research*, 26, 31–43.

Storey, J.D. (2011). False discovery rates. In: Lovric, M. (eds), *International Encyclopedia of Statistical Science*, Springer, pp. 504–508.

Takeuchi, T., Benning, C. (2019). Nitrogen-dependent coordination of cell cycle, quiescence and TAG accumulation in *Chlamydomonas*. *Biotechnology for Biofuels*, 12(292).

Wan Mahari, W.A., Wan Razali, W.A., Manan, H., Hersi, M.A., Ishak, S.D., Cheah, W., Chan, D.J.C., Sonne, C., Show, P.L., Lam, S.S. (2022). Recent advances on microalgae cultivation for simultaneous biomass production and removal of wastewater pollutants to achieve circular economy. *Bioresource Technology*, 364.

Wang, P., Grimm, B. (2021). Connecting Chlorophyll Metabolism with Accumulation of the Photosynthetic Apparatus. *Trends in Plant Science*, 5, 484–495.

Wang, Y., Stessman, D.J., Spalding, M.H. (2015). The CO2 concentrating mechanism and photosynthetic carbon assimilation in limiting CO2: How *Chlamydomonas* works against the gradient. *Plant Journal* 82, 429–448.

Wickham, H. (2016). *ggplot2: Elegant Graphics for Data Analysis* Second Edition. Springer-VerlagNew York.

Williams, S.P., Gillaspy, G.E., Perera, I.Y. (2015). Biosynthesis and possible functions of inositol pyrophosphates in plants. *Frontiers in Plant Science*, 6.

Willows, R.D., Lagarias, J.C., Duanmu, D. (2023). Tetrapyrrole biosynthesis and signaling (chlorophyll, heme, and bilins). In: *The* Chlamydomonas *Sourcebook: Volume 2: Organellar and Metabolic Processes*. Elsevier, pp. 691–731.

Wu, T., Wang, C., Han, B., Liu, Z., Yang, X., Wang, W., Ding, G., Hammond, J.P., White, P.J., Xu, F., Shi, L. (2023). Emerging roles of inositol pyrophosphates in signaling plant phosphorus status and phytohormone signaling. *Plant and Soil*.

Zhu, S., Yang, H., Bin, S., Wang, M., You, T., Li, X., Tian, L., Grossman, A.R., Lu, S., Yang, W. (2024). GreenCut protein LPB1 is required for SQDG accumulation and optimal photosynthetic electron transfer from QA− to QB in *Chlamydomonas reinhardtii*. *Algal Research*, 79.

Yin, M., Zhang, Z., Xuan, M., Feng, H., Ye, W., Zheng, X., Wang, Y. (2020). Conserved Subgroups of the Plant-Specific RWP-RK Transcription Factor Family Are Present in Oomycete Pathogens. *Frontiers in Microbiology*, 11, 1724.

Zúñiga-Burgos, T., Saiardi, A., Camargo-Valero, M.A., Baker, A. (2024). Phosphate overplus response in *Chlamydomonas reinhardtii*: Polyphosphate dynamics to monitor phosphate uptake and turnover. *Algal Research*, 81.

SUPPORTING INFORMATION

Additional supporting information can be found online in the Supporting Information section at the end of this article.

How to cite this article: Bedera-García, R., García-Gómez, M.E., Personat, J.M. & Couso, I. (2025) Inositol polyphosphates regulate resilient mechanisms in the green alga *Chlamydomonas reinhardtii* to adapt to extreme nutrient conditions. *Physiologia Plantarum*, 177(1), e70089. Available from: https://doi.org/10.1111/ppl.70089